COBEM 2023 27TH INTERNATIONAL CONGRESS OF MECHANICAL ENGENEERING

ABCM Brazilian Society of Mechanical Sciences and Engineering
27th ABCM International Congress of Mechanical Engineering
December 04-08, 2023, Florianópolis-SC, Brazil

COB-2023-0345
STRUCTURAL ANALYSIS OF AN ORE BELT CONVEYOR'S POLYMERIC ROLLER CONSIDERING VISCOELASTIC EFFECTS

Rafiq Said Dias Jabour
Marco Antônio Luersen
Department of Mechanical Engineering, Federal University of Technology – Paraná – UTFPR
Rua Deputado Heitor Alencar Furtado, 5000 – Cidade Industrial, Curitiba – PR, 81280-340
rafiqsaid@alunos.utfpr.edu.br, luersen@utfpr.edu.br

Abstract. *Belt conveyors are extensively employed in the mining industry for transporting ore. Rollers, also known as idlers, are cylindrical structures typically composed entirely of steel, providing support and guidance for the material above the belt. Incorporating an idler with an outer tube made of polymeric material offers advantages such as weight reduction and simplified manual part replacements by the maintenance operators. In this study, finite element models are built using the software Ansys to investigate the structural behavior of a roller with an outer tube made of high-density polyethylene (HDPE). The roller's design is evaluated based on the specifications and constraints outlined in the Brazilian standard ABNT NBR 6678. A typical characteristic of polymers is their viscoelastic behavior; hence, stress relaxation tests are performed on HDPE specimens to obtain material properties for incorporation into the numerical model. These tests are conducted following ASTM Practice D2991 and ASTM D638. A comparison between linear-elastic and linear-viscoelastic finite element models is carried out. The viscoelastic model exhibits a combination of instantaneous elastic response, viscous behavior, and residual deformation, truly representing the phenomena of viscoelasticity. Importantly, all stresses remained below the yield strength of their respective materials. Moreover, the viscoelastic model demonstrates a misalignment angle of the shaft in the bearings approximately 77% higher than that of the linear-elastic model. This discrepancy emphasizes the necessity and significance of incorporating viscoelastic properties to accurately modeling these types of rollers, as the misalignment angle of the shaft is a crucial factor affecting the performance of these components.*

Keywords: *belt conveyor roller, mechanical design, viscoelasticity*

1. INTRODUCTION

Belt conveyors play a crucial role in the mining industry as they facilitate the transportation of ore between crushing and sieving operations, and they also transport the ore to (or nearby to) ships or railway wagons. Rollers, also known as idlers, are cylindrical structures consisting of a tube that rotates freely around a fixed shaft. These components provide support and guidance for the material conveyed on the belt. Rollers are typically made entirely of steel, as specified in the Brazilian standard ABNT NBR 6678. This standard also defines the roller dimensions, the admissible load for each type of idler, maximum bending and shear stresses, as well as the maximum admissible misalignment angle of the shaft in the bearings (β). In mining operations, rollers endure high loads and harsh conditions, resulting in frequent component replacements during maintenance operations. These replacements are carried out manually, and the significant mass of the rollers can adversely affect the ergonomics and health of operators. Using polymeric materials in the manufacturing of the outer tubes is a way to decrease the roller's mass and alleviate this issue.

Polymers find various applications in the industry due to their moldability, recyclability, and ability to replace metals in machinery and equipment parts for weight reduction. High-density polyethylene (HDPE), the polymer used in the present study for the roller's outer tube, is a thermoplastic material that offers ease of processing and reasonable mechanical strength and stiffness. However, polymers present viscoelastic behavior. According to Canevarolo (2006), the viscoelastic behavior of polymers can be defined as a combination of fluidic and elastic properties. When polymers are subjected to loads, their mechanical properties vary over time. The viscoelasticity behavior is observed through two phenomena: creep and stress relaxation. Creep involves the gradual deformation of a specimen when subjected to a constant stress over time, while stress relaxation occurs when a constant deformation is applied, leading to a reduction in stress over time. By conducting creep and stress relaxation tests, we can understand how the mechanical properties of polymers change over time. These viscoelastic properties can then be incorporated into numerical models, enhancing their accuracy.

To analyze the mechanical behavior of loaded structures, finite element simulations are commonly employed. The finite element method (FEM) discretizes the continuum into a finite number of degrees of freedom, generating a system of equations that is numerically solved (Cook et al., 2001).

In this study, finite element models are built using the software Ansys to investigate the structural behavior of a roller with an outer tube made of HDPE. Two FEM models are considered: the first model assumes all materials as linear-elastic (similar to the study conducted by Ceniz et al., 2022), while the second model incorporates the viscoelastic properties of HDPE, which are experimentally determined through relaxation tests. The methodology is outlined in Section 2, where the material properties, boundary conditions, and other relevant details of the numerical models are defined. Section 3 presents the results, discussions, and a comparison between the responses of the linear-elastic and viscoelastic models. The main conclusions of the study are addressed in Section 4.

2. METHODOLOGY

This section outlines the methodology employed in the study. Firstly, the stress relaxation test procedure used to obtain the viscoelastic properties is presented. Subsequently, the steps to build the finite element model are described, along with relevant design details associated with the ABNT NBR 6678 standard for rollers.

2.1 Stress relaxation test

One of the numerical models analyzed in this study incorporates the viscoelastic effects of HDPE. The corresponding properties are obtained through stress relaxation tests conducted in accordance with ASTM D2991. This standard provides instructions for conducting the tests, including measurement definitions, control of vibration, temperature, and deformation. Additionally, ASTM D638 is referenced for selecting the specimen shape to be used. Figure 1 illustrates the dimensions of the HDPE specimen utilized in this study, which is referred to as Type I as per the aforementioned standard

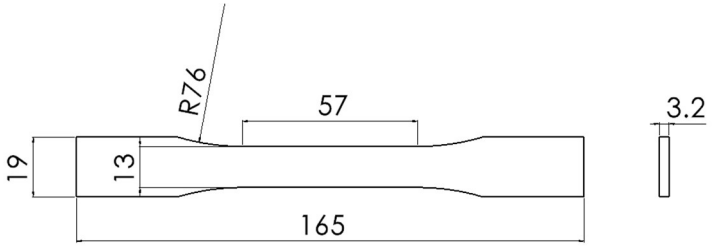

Figure 1. Dimensions (in mm) of Type I specimen, according to ASTM D638.

The test entails applying a constant deformation to the specimen using a tensile test machine (shown in Figure 2). The test begins with an initial force that keeps the specimen deformed, and the subsequent decrease in force over time, indicating stress relaxation, is recorded by the controlling equipment. Table 1 enumerates the key parameters considered in the test conducted for this study, which was performed at room temperature.

(a) (b)

Figure 2. HDPE stress relaxation test set-up: (a) overall view and (b) detail of the specimen and the clip-on strain gauge extensometer.

Table 1. HDPE stress relaxation test parameters.

Parameters	Value
Test duration time, s	3600
Grip deformation, mm	1.7
Gauge length deformation, mm	0.8
Strain	0.016
Data acquisition rate, points/s	5

By utilizing force versus time data, it becomes possible to calculate various material responses and properties, including the elastic and shear moduli. The normal stress can be determined using the following equation:

$$\sigma(t) = \frac{f(t)}{A}, \tag{1}$$

where A represents cross-sectional area of the specimen and $f(t)$ represents the force over time.

The longitudinal relaxation modulus can be calculated by (Siengchin and Rungsardthong, 2013):

$$E_r = \frac{\sigma(t)}{\varepsilon_0}, \tag{2}$$

where ε_0 is the constant strain given in Table 1. Then, the shear relaxation modulus G can be obtained by the isotropic relation:

$$G(t) = \frac{E_r}{2(1+\upsilon)}\,. \tag{3}$$

where υ is the Poisson's ratio.

The shear relaxation modulus data over time is incorporated into the FEM model as a viscoelastic property. Ansys employs the Prony series to derive the relative moduli and relaxation times from the shear modulus data. The shear relaxation modulus is expressed in terms of a Prony series (Chen, 2000) as follows:

$$G(t) = G_0\left[\alpha_\infty^G + \sum_{i=1}^{\eta_G} \alpha_i^G \exp\left(-\frac{t}{\tau_i^G}\right)\right], \tag{4}$$

where:

G_0= shear relaxation moduli at $t = 0$,
η_G= number of Prony terms,
α_i^G= relative moduli,
τ_i^G= relaxation time,
α_∞^G= relative moduli for long term ($t = \infty$).

The relative moduli α_i^G can be calculated by dividing the shear elastic moduli at current time G_i by the relaxation shear modulus at time $t = 0$:

$$\alpha_i^G = \frac{G_i}{G_0}\,. \tag{5}$$

To insert data obtained by Eq. (3) in the numerical model, the following steps should be followed:

1- Input "Shear Data – Viscoelastic" and "Prony Shear Relaxation" properties in "Engineering Data";
2- Insert relaxation shear modulus over time in the spreadsheet fields;
3- Choose the number terms of the Prony series;
4- Fit the curve in the Prony Shear Relaxation property and select the command to copy the calculated values. This command calculates the terms of the Prony series through a fitting procedure.

In the numerical model employed in this study, 63 points are inserted for the shear relaxation modulus and their corresponding time instant. After that, 10 terms of the Prony series are calculated, and their values are presented in Table 2.

Table 2. HDPE's Prony shear relaxation terms - Ansys FEM model's viscoelastic property.

Relative moduli	Relaxation time, s
0.043886	13.96
0.066908	56.049
0.041133	322.82
0.063637	55.331
0.044182	322.83
0.044095	322.83
0.044588	3.2132
0.070114	3380.2
0.069911	3377.8
0.042205	2964

2.2 Finite element models

Commonly, the initial step in constructing a finite element model (FEM) is defining the material properties. Figure 3 provides an overview of the materials used for each component of the idler structure, which can be summarized as follows: an outer tube composed of HDPE, a shaft made of AISI 1020 steel, and bearing seats (inner tube structures that house the bearings) made of polyamide 6 (PA.6), commonly referred to as nylon.

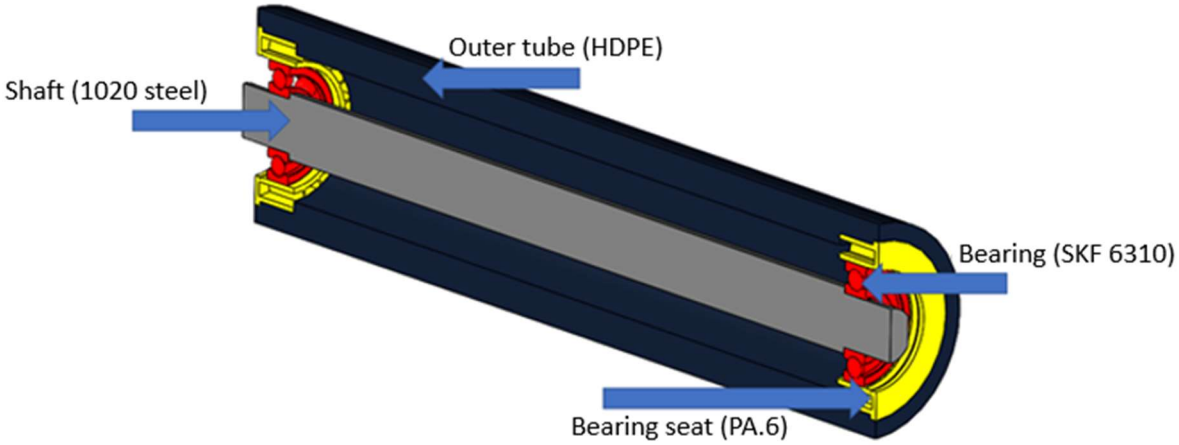

Figure 3. Polymeric roller – parts and materials.

The material specifications for the shaft and bearings are defined in accordance with ABNT NBR 6678, and their key mechanical properties are presented in Table 3. In this table, only elastic properties are listed, as the viscoelastic properties is discussed in subsection 2.1.

Table 3. Materials properties.

Property (symbol)	Structural steel (shaft)	HDPE (outer tube)	PA.6 (bearing seats)
Density (ρ), kg/m^3	7850	961	1140
Elasticity modulus (E), GPa	210	0.51573	1.11
Poisson's ratio (ν)	0.30	0.46	0.35
Yield strength (σ_y), MPa	250	28	43.13
Ultimate strength (σ_R), MPa	460	30	71.89

After defining all the materials, the next step in constructing the numerical model is to adjust the geometry of the analyzed structure. To reduce the computational cost of the simulation, a symmetry region is considered in the central transversal plane (YZ plane), as illustrated in Figure 4.

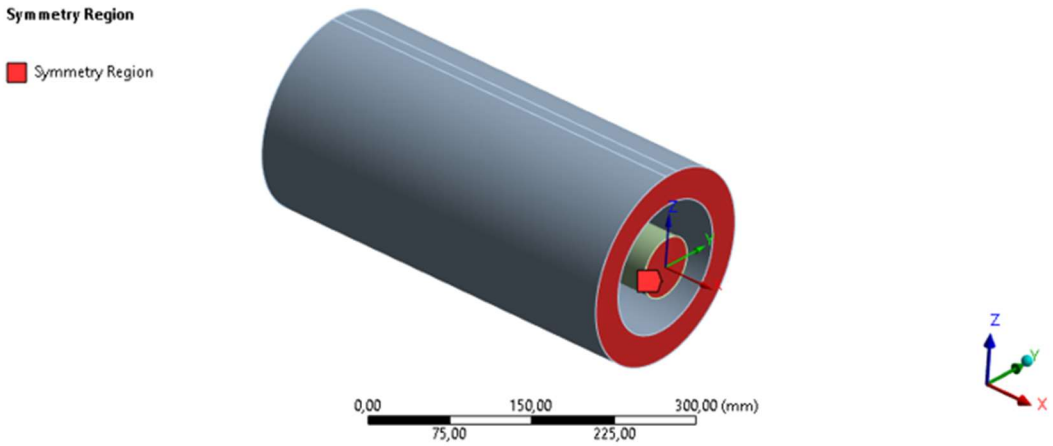

Figure 4. Symmetry region on plane YZ created in the idler's numerical model (Red means the region where were applied the symmetry conditions).

The bearings in the model are represented by spring-damper elements generated using the SKF Bearing App, an Ansys Workbench-compatible extension. According to the ABNT NBR 6678 standard, bearing 6310 is recommended for rollers with an outer tube diameter ranging from 178 mm to 203 mm and a shaft series of 50 (where the series number corresponds to the diameter in millimeters in the bearing contact region). To incorporate the bearing element using the SKF extension, it is necessary to establish a coordinate system within the bearing track, define the outer and inner faces involved in the bearing contact, and specify the bearing code, which, in this case, is 6310. Figure 5 provides an illustration of these characteristics in the numerical model.

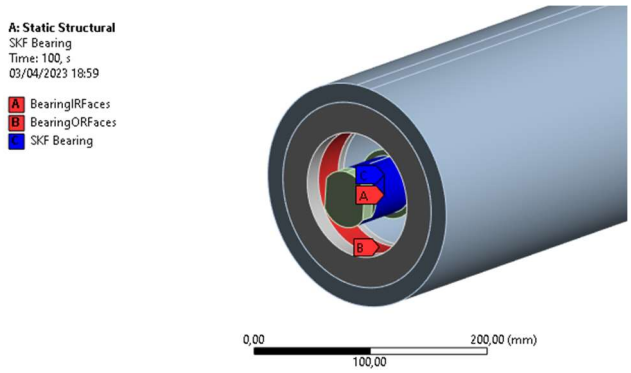

Figure 5. Bearing element created by SKF Bearing App.

Another crucial step in the pre-processing phase is the generation of the mesh. In this study, the Hex Dominant method is employed to create the mesh, utilizing a combination of hexahedral and tetrahedral elements with an average size of 10 mm. Additionally, the boundary conditions, including load and constraints should be inserted. The ABNT NBR 6678 standard provides guidelines for determining the minimum allowable load for rollers based on factors such as the idler's length, shaft series, and roller type (e.g., carrying, return, or impact; single, with two, or three rollers). The roller analyzed in this study is classified as a carrying triple idler, measuring 800 mm in length and belonging to series 50, resulting in a minimum allowable load of 15817 N. To apply the load to the structure, a 15 mm wide area is projected onto the outer tube's surface. This value is determined using Hertz's equations presented by Johnson (1985). As shown in Figure 6, a load of 7908.5 N is applied to the surface, which represents half of the total load due to the presence of symmetry. Furthermore, the figure shows the constraints at the shaft's extremity, limiting translations along all axes and rotations around the X and Z axes. Rotation around the Y axis is permitted to account for shaft bending under load.

It is important to mention that, although the actual problem involves dynamic effects and loads resulting from the rotation of the roller, static analyses are performed in this study. This choice is based on the fact that the main excitation frequency, i.e., the roller's rotational speed (500 rpm / 8.33 Hz), is far from the fundamental frequencies of the system. Moreover, the design follows the static considerations outlined in a standard code.

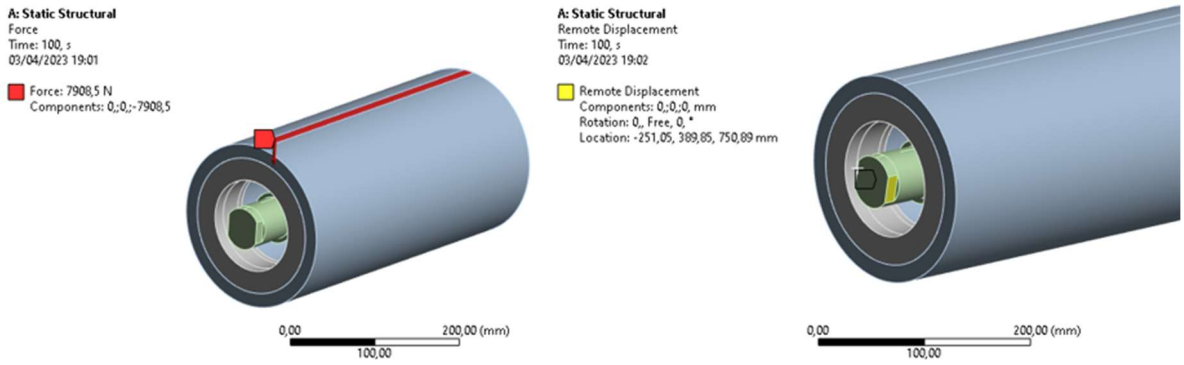

Figure 6. Boundary conditions: load and constraints.

2.3 Analysis details

In this study, both linear and viscoelastic analyses are conducted. Initially, the linear simulation is performed to assess the model characteristics as mesh, boundary conditions and loads, and understand the behavior of the structure without accounting for viscoelastic effects. This approach requires less computational time. Subsequently, the viscoelastic model is simulated, considering the properties obtained from the stress relaxation test. To visualize the corresponding behavior in the simulation, the force is applied in defined load steps, as presented in Table 4.

Table 4. Load steps.

Step	**End time, s**	**Force,** N
0	0	0
1	5	7908.5
2	360	7908.5
3	720	7908.5
4	1080	7908.5
5	1800	7908.5
6	2160	7908.5
7	2520	7908.5
8	2880	7908.5
9	3240	0
10	3600	0

The misalignment angle between the shaft and the bearings is calculated by

$$\beta = \tan^{-1}\left[\frac{(\Delta_{z1}-\Delta_{z2})-(\Delta_{z3}-\Delta_{z4})}{L}\right]\cdot\frac{180^\circ}{\pi}\cdot\frac{60\prime}{1^\circ}, \tag{6}$$

where L is the bearing track length, which is equals to 27 mm, and the terms Δ_{z1}, Δ_{z2}, Δ_{z3}, and Δ_{z4} are the displacements in the Z-axis of the points showed in Figure 7.

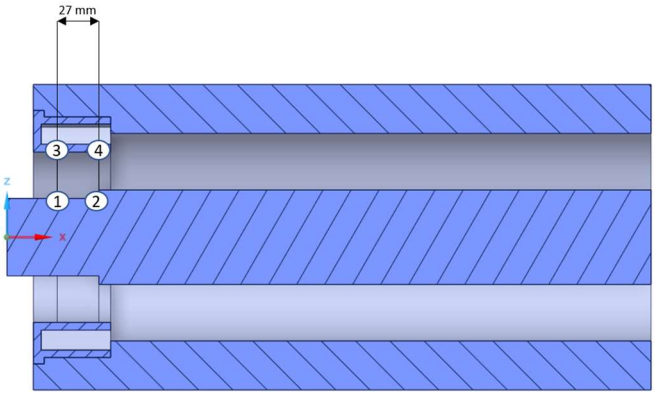

Figure 7. Control points where displacement is obtained to calculate the β angle.

3. RESULTS AND DISCUSSION

This section presents the results obtained from the stress relaxation tests conducted on HDPE specimens, as well as the results of the finite element simulations performed on the roller. Additionally, a comparison is made between the responses of the linear-elastic and viscoelastic models.

3.1 HDPE stress relaxation test results

The tensile test machine's load cell records the force data over time. Figure 8 illustrates the stress relaxation test curve. Then, by applying Eqs. (1), (2), and (3), the shear relaxation modulus can be determined (see Figure 9).

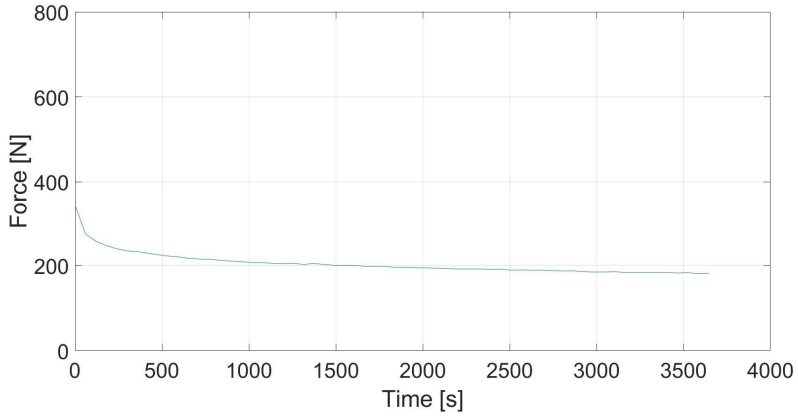

Figure 8. Force *versus* times recorded during the HDPE relaxation test.

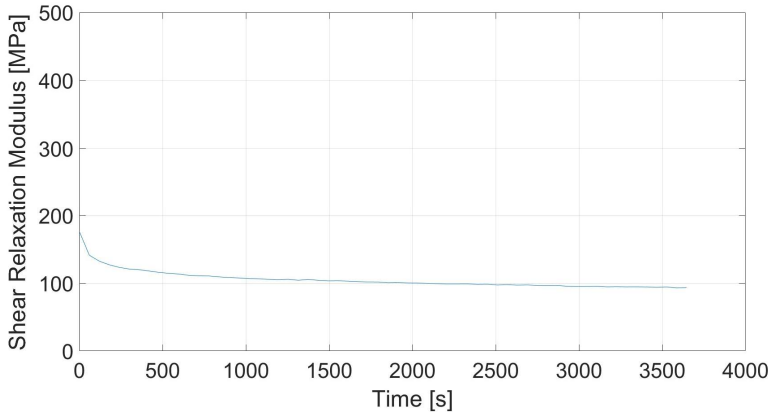

Figure 9. HDPE shear relaxation modulus.

3.2 Numeric models results

The responses related to stresses, deformations and the angle of misalignment between the shaft and the bearings are obtained from the results of the finite element models simulations. Figure 10 illustrates the von Mises stress responses in the shaft at the moments when the stresses reach their peak values. It can be seen that the highest stress levels are concentrated in the constrained region (where the shaft is supported) for both the linear-elastic and viscoelastic models. In the middle of the structure, specifically at the symmetry plane, the stress level is approximately 13 MPa for the linear-elastic model and 20 MPa for the viscoelastic model. These values are significantly lower than the yield strength of the respective material (250 MPa).

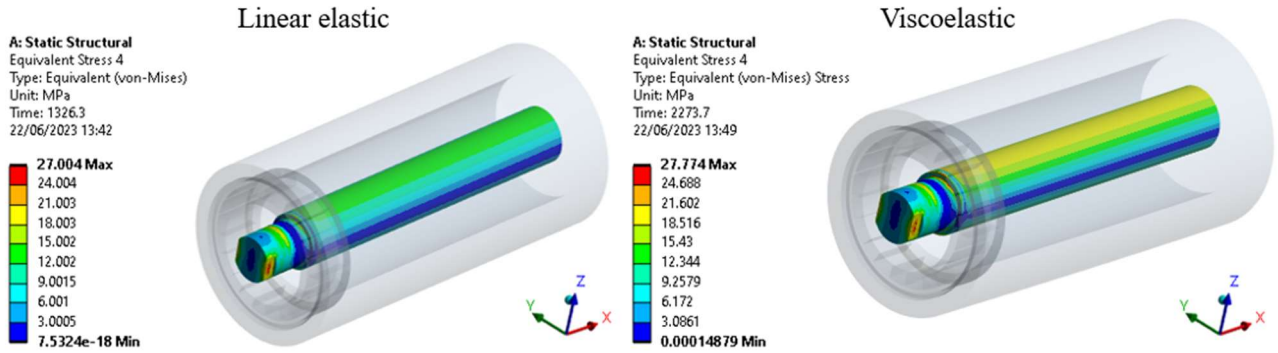

Figure 10. Von Mises stress responses in the steel shaft in the linear-elastic and viscoelastic models.

Figure 11 illustrates the stress responses of the roller's outer tube during the load steps defined in subsection 2.3. In the viscoelastic model, the stress increases over time despite the constant applied force, unlike the linear-elastic model, which reaches a plateau and remains constant until the load is released. Additionally, there is residual stress observed in the viscoelastic analysis.

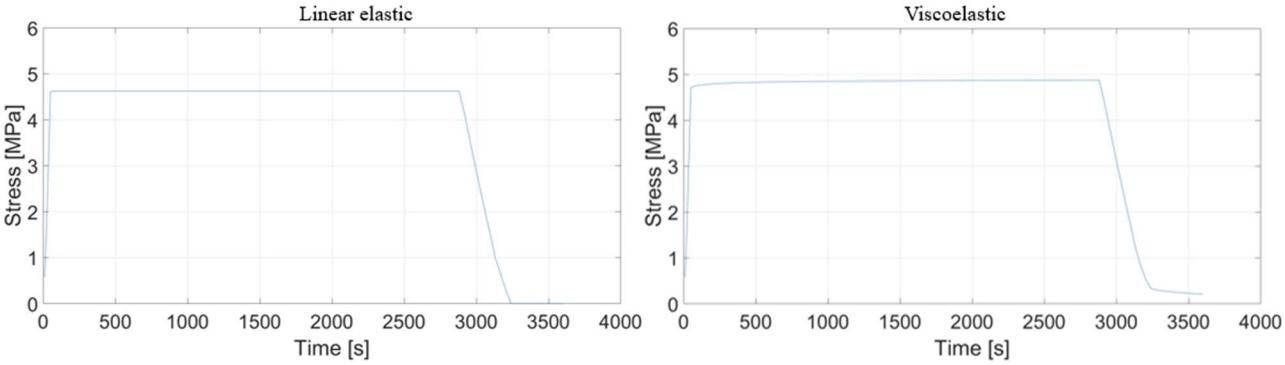

Figure 11. Maximum stress response in the outer tube (linear-elastic and viscoelastic models).

Figure 12 illustrates the deformation in the Z-axis of the outer tube over time. In the viscoelastic model, the deformation increases throughout the load steps, resembling the behavior observed in a creep, following a non-linear curve. While the linear model shows a maximum deformation of 4.1 mm, the viscoelastic model reaches 6.45 mm.

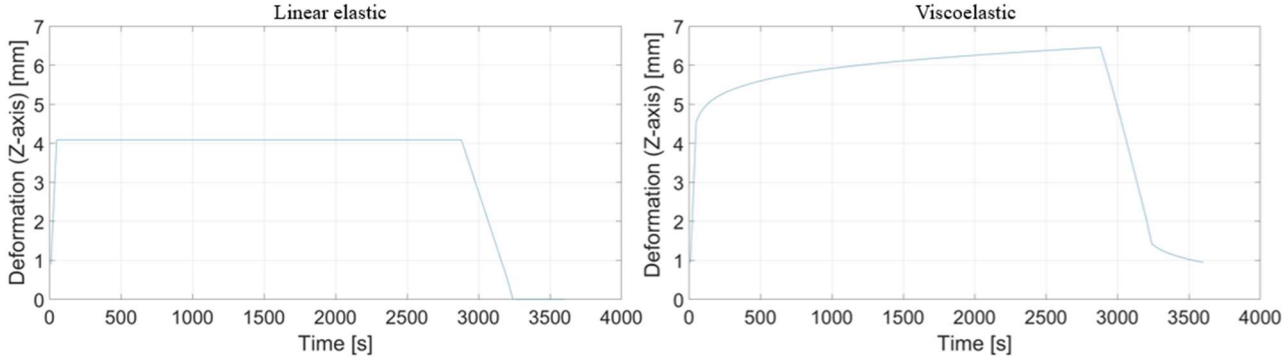

Figure 12. Maximum directional deformation response in the outer tube (linear-elastic and viscoelastic models).

The most significant difference observed among the parameters is the angle β. There is an approximate 77% disparity between the linear model (21.9') and the viscoelastic model (38.7'). It is worth noting that the misalignment in both models exceeds the threshold defined by the ABNT NBR 6678 standard. According to the standard, the maximum allowable misalignment for carrying idlers is 9'. Figure 13 presents the response of angle β for both models.

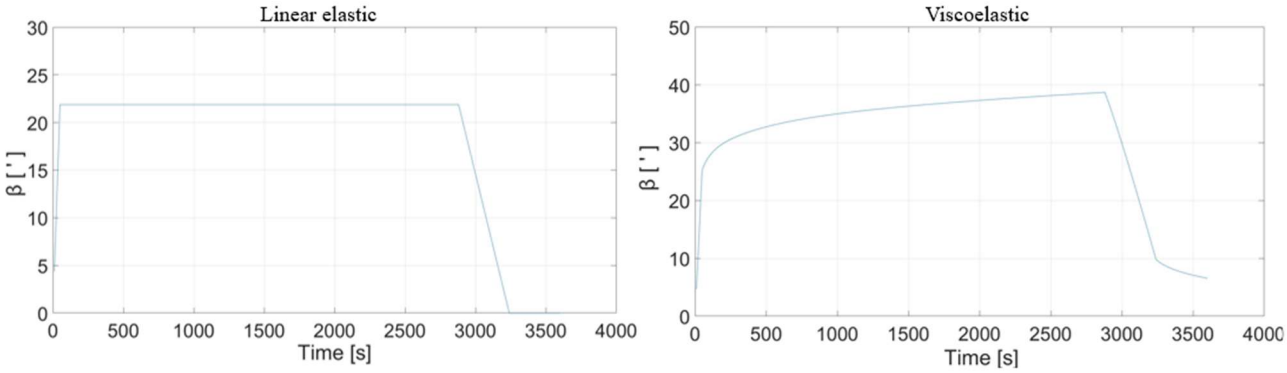

Figure 13. Angle of misalignment between the shaft and the bearings (linear-elastic and viscoelastic models).

4. CONCLUSIONS

Based on the results presented in Section 3, it can be concluded that incorporating viscoelasticity into the simulation leads to higher computational costs; however, it brings the numerical model closer to reality. The results of the models presented here demonstrate that the viscoelastic effect directly influences the structural responses, including stress and deformation of the parts. The curves depicting these parameters over time exhibit behavior similar to that observed in fundamental mechanical tests of polymers, specifically the creep test, where the specimen is subjected to constant stress and its deformation increases over time. Additionally, the remaining deformation and stress in the structure resemble the behavior predicted by the Maxwell-Voigt model, which is commonly used to explain viscoelastic phenomena in polymers. Consequently, the model effectively represents the behavior of polymers, which is valuable for understanding the mechanical behavior of polymeric idlers and preventing future design issues such as misalignment between the shaft and bearings. High misalignment adversely affects bearing performance, leading to failure. Therefore, modifying the polymer stiffness can improve this parameter.

5. ACKNOWLEDGEMENTS

The authors would like to thank Vale S.A. Company and the Institute of Technology Vale (ITV) for sponsoring this research through Project No. SAP 4600048682.

6. REFERENCES

ABNT NBR 6678, 2017. *Continuous mechanical handling equipments - Belt conveyors - Idlers - Design, selection and standardization* (*in Portuguese*). Associação Brasileira de Normas Técnicas (ABNT), Rio de Janeiro, RJ, Brazil.

ASTM D2991, 1984. *Standard Practice for Testing Stress-Relaxation of Plastics*. American Society for Testing and Materials (ASTM International), West Conshohocken, PA, USA.

ASTM D638, 2002. *Standard Test Method for Tensile Properties of Plastics.* American Society for Testing and Materials (ASTM International), West Conshohocken, PA, USA.

Canevarolo Jr, S.V., 2006. *Science of Polymers* (*in Portuguese*)*,* second edition. Artliber Editora Ltda, São Paulo, SP, Brazil.

Ceniz, J.P., Martins, R.S., Luersen, M.A. and Cousseau, T., 2022. "Structural Optimization of Metal and Polymer Ore Conveyor Belt Rollers". *Computer Modeling in Engineering & Sciences*, Vol. 133, p. 601-618.

Chen, T., 2000. *Determining a Prony Series for a Viscoelastic Material from Varying Time Strain Data*. National Aeronautics and Space Administration. Langley Research Center Hampton, Virginia 23681-2199.

Cook R.D., Malkus, D.S., Plesha, M.E. and Witt, R.J., 2001, *Concepts and Applications of Finite Element Analysis*, fourth Edition. John Willey and Sons, New York, NW, USA.

Johnson, K. L., 1985. *Contact mechanics*. First Edition. Cambridge University Press, Cambridge, UK.

Siengchin, S. and Rungsardthong, V., 2013. "HDPE reinforced with nanoparticle, natural and animal fibers: Morphology, thermal, mechanical, stress relaxation, water absorption and impact properties". *Journal of Thermoplastic Composite Materials*, Vol. 26, p. 1025-1040.

7. RESPONSIBILITY NOTICE

The authors are the only responsible for the printed material included in this paper.